PHYSICAL REVIEW E **73**, 020403(R) (2006)

Dynamic signature for the equilibrium percolation threshold of attractive colloidal fluids

Samartha G. Anekal,[1] Pradipkumar Bahukudumbi,[2] and Michael A. Bevan[1,*]
[1]*Department of Chemical Engineering, Texas A&M University, College Station, Texas 77843-3122, USA*
[2]*Department of Mechanical Engineering, Texas A&M University, College Station, Texas 77843-3123, USA*
(Received 3 July 2005; revised manuscript received 19 December 2005; published 23 February 2006)

Short-time self-diffusivities, D_S^S, are computed for attractive colloidal fluids with van der Waals potentials to identify their percolation threshold and a previously unexplained dynamic transition. Our results show a discontinuous change in the slope of D_S^S vs temperature as the percolation threshold is crossed. Because D_S^S depends only on multibody hydrodynamic interactions, the percolation threshold of attractive colloidal fluids is shown to correspond to a transition in a dynamic property consistent with the linear viscoelastic measurements of Woutersen *et al.*, J. Chem. Phys. **101**, 542 (1994).

DOI: 10.1103/PhysRevE.73.020403 PACS number(s): 82.70.Dd, 64.60.Ak, 82.70.Gg, 83.10.Mj

Attractive colloidal particles form equilibrium and nonequilibrium microstructures determined by their concentration and the magnitude and range of their attraction. For weak attraction, single-phase fluids and coexisting gas-liquid and liquid-solid phases are observed, whereas strong attraction produces irreversible fractal gels [1]. Elevated attraction and concentration can also produce dynamically arrested microstructures [2]. Whether colloidal attraction originates from van der Waals, depletion, or biomolecular interactions, controlled assembly of attractive colloids into useful microstructures requires the ability to intelligently manipulate particle interactions and dynamics to navigate free energy landscapes in such systems.

To begin to understand the importance of multibody hydrodynamic interactions in colloidal assembly processes, here we investigate dynamical changes as the equilibrium percolation threshold (PT) is crossed, which is one of the simplest structural transitions of weakly attractive colloids. The equilibrium PT is defined to occur when attractive colloids produce system spanning clusters in half of all configurations. The PT is not a phase transition since it is not accompanied by discontinuous changes in thermodynamic quantities or their derivatives, but is a distinctive feature in an otherwise barren landscape of single-phase fluid configurations with insufficient concentration or attraction to produce coexisting equilibrium phases, arrested glasses, or irreversible gels.

Although the PT is one of few notable features on kinetic pathways from initially hard sphere fluids towards gel, glass, and crystal structures at higher particle attractions and concentrations, changes in relaxation mechanisms and frequency-dependent properties of colloidal fluids across the PT are not yet fully understood. Numerous studies have investigated attraction and concentration dependent rheological transitions in colloidal fluids with temperature-dependent pair potentials but have focused primarily on the fluid-gel transition beyond the PT [3–5]. Experimental studies of dynamical changes across the PT are generally complicated by having to measure linear viscoelastic properties and also having an independent measurement of the percentage of system spanning clusters averaged over space and time. Although much theoretical work has been dedicated to consistently treating thermodynamic and hydrodynamic relaxation mechanisms in repulsive colloidal fluids [6], similar approaches have not been extended to attractive colloidal fluids in the vicinity of their PT.

Here we report evidence of a dynamic signature of the equilibrium PT of attractive colloid fluids that is dominated by multibody hydrodynamic interactions. In particular, we observe a discontinuous rate of change in the short-time self-diffusivity, D_S^S, vs temperature, T, for polymer coated colloids with realistic van der Waals (vdW) potentials at a locus of conditions nearly identical to the PT of adhesive spheres (AS) with equivalent second virial coefficients, B_2. This dynamic signature serves as a criterion for the equilibrium PT of attractive colloids and provides new insights into the role of multibody, dissipative hydrodynamic interactions in the structural evolution of attractive, single-phase, equilibrium colloidal fluids. The predicted change in D_S^S across the percolation threshold is consistent with, and can be used to explain, the linear viscoelastic measurements of attractive colloidal fluids by Woutersen *et al.* [7].

This investigation is motivated by our previous measurements of a T and concentration-dependent transition of polystyrene (PS) colloids (radius, $a=180$ nm) with adsorbed polyethylene oxide-polypropylene oxide-polyethylene oxide (PEO-PPO-PEO) (thickness at 25 °C, $\delta=20$ nm) in aqueous 0.5 M NaCl [8] for which the potential is well known [9]. Figure 1 shows a phase diagram for such polymer-coated particles as a function of T and a PS core particle volume fraction, ϕ_{core}. With increasing T, the net attraction is mediated by diminishing solvent quality for the PEO moieties. The pair potential between such particles (hereafter referred to as the vdW potential) can be modeled to include a hard-wall repulsion that collapses with increasing T and a van der Waals attraction between core particles and solvated copolymer coatings. By equating B_2's for the vdW and AS potentials (to link T and the AS parameter τ), Fig. 1 is constructed to show AS predictions for gas-liquid coexistence and the critical point [8], liquid-solid coexistence [10], the PT [11,12], and glass lines [2]. The phase diagram appears in-

*Electronic address: mabevan@tamu.edu

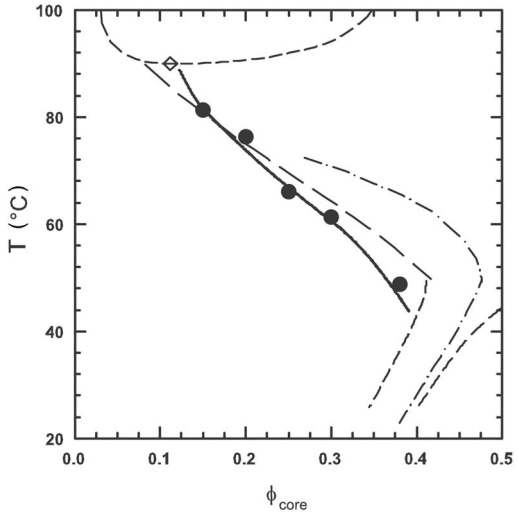

FIG. 1. Phase diagram showing gas-liquid and liquid-solid coexistence (– –) and critical point (◇); percolation thresholds from MC simulations (—) [11], theory (— —) [12], and transitions in short time self-diffusivity (●); glass lines (— ·) [2].

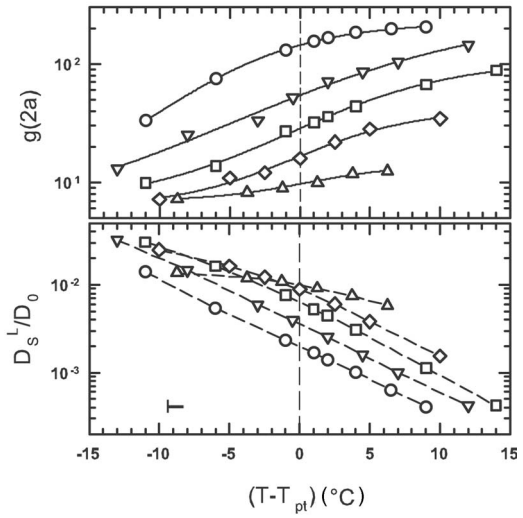

FIG. 2. Pair distribution function at contact (top) and normalized long-time self-diffusivity (bottom) for MC simulations of colloids with temperature-dependent vdW potentials. Data plotted on temperature scale relative to equivalent AS PT for $\phi_{core}=0.15$ (○), 0.20 (▽), 0.25 (□), 0.30 (◇), and 0.38 (△). Also shown are fits using Eq. (1) (—) and lines to guide the eye (– –).

verted due to the lower critical solution temperature of the adsorbed copolymer in aqueous media.

To understand how structural relaxations change as the PT is approached and traversed with increasing attraction in equilibrium colloidal fluids, we performed standard canonical (*NVT*) Monte Carlo (MC) simulations for copolymer coated particles interacting via the vdW potential. Equilibrium configurations for 108 and 256 particles were generated for a range of T and ϕ_{core} values bounding the AS PT in Fig. 1.

Before examining dynamic quantities, we first establish that the MC simulated equilibrium fluid configurations display the expected continuous changes in thermodynamic properties via the pair distribution function at contact, $g(2a,\phi)$, in Fig. 2. Results are shown for the five MC simulated ϕ_{core} values on a temperature scale relative to the equivalent AS PT temperature, T-T_{pt}. The MC simulated values of $g(2a,\phi)$ are well represented by the solid lines in Fig. 2 given by

$$g(2a_{eff},\phi_{eff}) = g_{HS}(2a_{eff},\phi_{eff})\exp[-u_{vdW}(2a_{eff})/kT] \quad (1)$$

which is the hard sphere radial distribution function at contact [13] times a Boltzmann factor for the vdW potential at contact based on effective radii ($a_{eff}=a+\delta$) and volume fractions [$\phi_{eff}=\phi_{core}(a_{eff}/a)^3$]. The data and fits in Fig. 2 display smooth changes in $g(2a,\phi)$, confirming the absence of any thermodynamic transitions across the equivalent AS PT.

Next, we compute short-time, D_S^S, and long-time, D_S^L, self-diffusivities for the MC simulated fluid configurations in Fig. 2. Values of D_S^S are computed from the trace of the N-particle diffusion tensor, **D**, as

$$D_S^S = \frac{1}{3N}\left\langle \sum_{i=1}^{3N} D_{ii} \right\rangle, \quad (2)$$

where the brackets indicate an average over all configurations for each set of T, ϕ_{core} conditions. **D** is related to the resistance tensor, **R**, through the generalized Stokes-Einstein relation, $\mathbf{D}=kT\mathbf{R}^{-1}$. Here **R** is computed using the method of Brady and Bossis [14], where hydrodynamic interactions are separated into far-field, multibody, and near-field lubrication contributions as

$$\mathbf{R} = (\mathbf{M}^{\infty})^{-1} + \mathbf{R}_{2B} - \mathbf{R}_{2B}^{\infty}, \quad (3)$$

where $\mathbf{M}^{\infty}$ is the far-field mobility tensor constructed in a pairwise manner. The inverse of $\mathbf{M}^{\infty}$ is a true multibody, far-field approximation to the resistance tensor. Lubrication is included by adding the exact two-particle resistance tensor [15], $\mathbf{R}_{2B}$, and subtracting the two-body, far-field resistance tensor, $\mathbf{R}_{2B}^{\infty}$, to avoid double counting.

To demonstrate the accuracy of Eqs. (2) and (3) for attractive equilibrium colloidal fluids before applying them to all MC simulated configurations, we compare them with mean-squared displacements (MSD), $\langle \Delta r^2(\Delta t)\rangle$, obtained from Stokesian Dynamic (SD) simulations. SD simulations were performed using the Langevin equation as [16]

$$\mathbf{r} = \mathbf{r}^0 + kT(\nabla\cdot\mathbf{R}^{-1})\Delta t + \mathbf{R}^{-1}\cdot\mathbf{F}^P\Delta t + \mathbf{X}(\Delta\mathbf{t}), \quad (4)$$

where **r** is the $3N$ particle coordinate vector, $\mathbf{F}^P$ is the net conservative force vector, and **X** is the random Brownian displacement such that $\langle\mathbf{X}\rangle=\mathbf{0}$ and $\langle\mathbf{XX}\rangle=2kT\mathbf{R}^{-1}\Delta t$. The time step, Δt, was chosen to be larger than the momentum relaxation time, $\tau_B=m/(6\pi\mu a)$, but smaller than the diffusive time, $\tau_D=a^2/D_0$, where $D_0=kT/(6\pi\mu a)$ is the single particle Stokes-Einstein diffusivity.

Using the final MC simulated configuration at $T=70$ °C, $\phi_{core}=0.25$ as the initial configuration in an SD simulation, Fig. 3 shows a solid line for MSD vs time by averaging over multiple time origins and all particles ($N=108$). The dashed line intercepting the origin and tangential to the MSD at

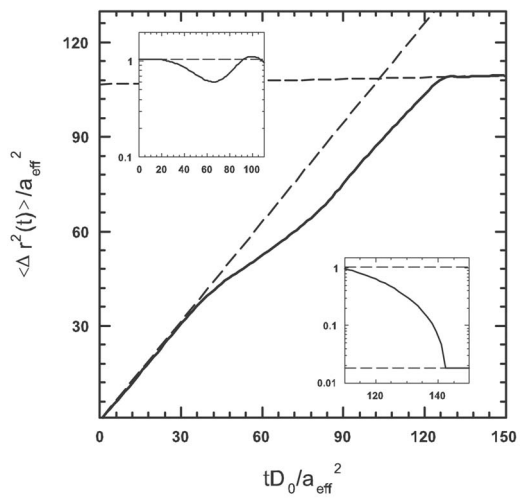

FIG. 3. MSD and its derivative (insets) vs time from SD simulations (—) at $T=70$ C, $\phi_{core}=0.25$. Short-time [Eq. (2)] and long-time [Eq. (5)] diffusivities predicted from MC simulated configurations (– –) at the same conditions.

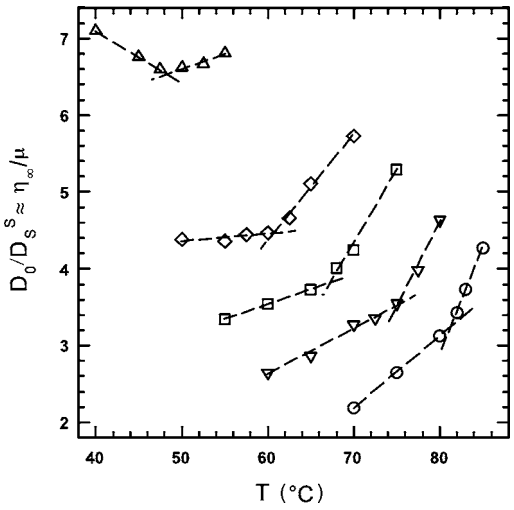

FIG. 4. Reciprocal of normalized short-time self-diffusivity vs temperature for $\phi_{core}=0.15$ (○), 0.20 (▽), 0.25 (□), 0.30 (◇), and 0.38 (△). Linear fits shown to guide the eye (– –).

short times has a slope of $6(D_S^S/D_0)$ where D_S^S was computed using Eqs. (2) and (3) by averaging over all MC simulated configurations at $T=70$ °C, $\phi_{core}=0.25$. The dashed line tangential to the linear region at long times has a slope of $6(D_S^L/D_0)$ where [6]

$$D_S^L = D_S^S[1 + 2\phi_{eff}g(2a_{eff}, \phi_{eff})]^{-1}, \quad (5)$$

and $g(2a, \phi_{eff})$ and D_S^S are computed using Eqs. (1)–(3). Insets in Fig. 3 show derivatives of MSD vs time as solid lines and values of $6(D_S^S/D_0)$ and $6(D_S^L/D_0)$ from MC simulations as dashed lines.

Figure 3 displays excellent agreement between D_S^S and D_S^L obtained from SD simulations and predictions from Eqs. (1) and (5) with MC simulated configurations. The agreement of diffusivities determined independently from MC and SD simulations confirm that equilibrium colloidal fluids are retained beyond the PT and that D_S^S and D_S^L can be accurately predicted from MC simulations without performing computationally expensive dynamic simulations. D_S^S has a known system size dependence in Eq. (2) [17] that can be corrected using [18]

$$D_S^S(\infty) = D_S^S(N) + D_0\mu/\eta[1.7601(\phi/N)^{1/3} - (\phi/N)], \quad (6)$$

where $D_S^S(\infty)$ is the infinite system size value, $D_S^S(N)$ is the N-particle value, and μ and η are the medium and dispersion viscosities. Because simulations were performed for $N=108$ and $N=256$, $D_S^S(\infty)$ could be obtained without independently determining μ/η.

Using Eqs. (2), (5), and (6), D_S^S and D_S^L were computed for MC simulated configurations of vdW particles for all conditions investigated in Fig. 2. To demonstrate the smooth variation of D_S^L across the PT (similar to molecular fluids), Fig. 2 shows D_S^L vs T-T_{pt}. For comparison, Fig. 4 shows a plot of D_0/D_S^L vs T for different ϕ_{core}. Each ϕ_{core} set displays a pronounced slope change at temperatures estimated from the intersection of linear fits to high and low temperature regions. The resulting transition temperatures for each ϕ_{core} set (plotted in Fig. 1) indicate a dynamic transition of vdW particles nearly identical to the equivalent AS PT. As a result, the PT of vdW particles appears to have a dynamic signature determined exclusively by multibody hydrodynamic interactions contained in D_S^S in Eq. (2).

An advantage of identifying the PT from changes in D_0/D_S^S is its direct connection to linear viscoelastic properties in attractive colloidal fluids. Because D_0/D_S^S is proportional to the high frequency dynamic viscosity, η_∞/μ, [6] the results in Fig. 4 predict an abrupt rate of change in η_∞/μ vs T at the PT of attractive colloidal fluids that can be compared with experimental measurements. This prediction appears to be consistent with the unique high frequency, linear viscoelastic measurements of an attractive colloidal fluid (octadecyl coated silica in benzene) by Woutersen *et al.* [7]. By fitting a general Maxwell model to their dynamic viscosity measurements in the range 70–250,000 Hz, Woutersen *et al.* found an abrupt change in the dependence of the relaxation time, a^2/D_S^S, vs T at the PT. Our results in Fig. 4 suggest the mechanism for their observed transition in a^2/D_S^S vs T is based on changes in multibody hydrodynamic interactions as the PT is crossed.

Although D_S^S is a measure of local particle mobility, it is important to note that it critically depends on both near-field, lubrication and far-field, multibody interactions. In fact, inclusion of multibody, far-field interactions is essential to the proper prediction of D_S^S to obtain even qualitative agreement with experiments [17]. Because D_S^S has a unique multibody dependence on particle configurations that is distinct from the pairwise dependence of $g(r)$, it is possible to have a dynamic transition determined by dissipative interactions at the PT in Fig. 1 for conditions where pairwise conservative interactions produce no thermodynamic transition. Values of D_S^S computed by considering only pairwise lubrication interactions between adjacent particles are not expected to capture the transition in Fig. 4.

It should be noted that the transition in D_0/D_S^S vs T in

Fig. 4 across the percolation threshold occurs within the single-phase fluid region of Fig. 1 and does not indicate a fluid-solid transition associated with gelation or dynamic arrest [3–5]. Although D_S^S contributes to $\eta(\omega)/\mu$ at all frequencies based on its dominance at the high frequency limit ($D_S^S \sim \eta_\infty^{-1}$) and finite contribution to D_S^L [Eq. (5)] in the zero frequency limit ($D_S^L \sim \eta_0^{-1}$), the smooth variation of D_S^L across the PT in Fig. 2 indicates that the low frequency dynamic viscosity, η_0/μ, should not display any discontinuous changes indicative of gelation or dynamic arrest [4,5]. Thus, the discontinuous rate of change in D_S^S vs T in Fig. 4 is a dynamic signature of the PT only and does not indicate a fluid-gel transition that is expected beyond the PT [3].

Although our simulated results in Fig. 4 are consistent with the high frequency measurements of Woutersen *et al.*, it is not obvious how the complete spectrum of relaxation times varies across the PT. The inverse relationship between dynamic viscosity and self-diffusivity should allow prediction of the normalized viscosity $[\eta(\omega)-\eta_\infty]/(\eta_0-\eta_\infty)$, in terms of the normalized self-diffusivity, $[1/D_s(\omega)-1/D_S^S]/(1/D_S^L-1/D_S^S)$, vs the nondimensional frequency, $\omega a^2/D_S^S$ [6]. Another issue when comparing our results with rheological experiments is the possibility of departures from equilibrium. Our results may be valid for small perturbations to equilibrium structures, but additional multibody hydrodynamic contributions may be expected to affect relaxation times in nonequilibrium colloidal fluids [19].

A final issue worth noting is the benefit of identifying the PT using the dynamic criterion based on its applicability to particles with continuous potentials such as the vdW attraction examined here. For the inverse power law decay of vdW potentials, an arbitrary cutoff separation must be specified to identify connectedness, clusters, and the PT in particle configurations. For comparison, particles with discontinuous AS and square-well potentials form unambiguous "bonds" for separations within their attractive wells. However, by observing changes in D_0/D_S^S at a locus of T, ϕ_{core} conditions, we recover a PT for vdW particles nearly identical to equivalent AS particles with a clearly identifiable PT. The dynamic signature of the PT provides a means to avoid the connectedness issue. Reanalyzing our data with knowledge of the PT also indicates that a unique cutoff separation does not exist for the vdW potential.

In conclusion, we report evidence of a dynamic transition at the equilibrium PT of attractive colloidal fluids based on a discontinuous rate of change in D_0/D_S^S vs T data for a range of ϕ_{core} values. Our results indicate a dynamic signature for the PT that is consistent with the rheological measurements of Woutersen *et al.* [7]. Extension of these findings might provide insights into the combined roles of multibody, dissipative and pairwise, conservative interactions for other colloidal structural transitions, particularly for colloids with different effective thermodynamic and hydrodynamic sizes.

We thank David M. Ford for useful discussions. Financial support was provided by a NSF PECASE (Grant No. CTS-0346473) and the ACS Petroleum Research Fund (Grant No. 41289-G5).

[1] W. B. Russel, D. A. Saville, and W. R. Schowalter, *Colloidal Dispersions* (Cambridge University Press, New York, 1989).
[2] L. Fabbian *et al.*, Phys. Rev. E **59**, R1347 (1999).
[3] M. C. Grant and W. B. Russel, Phys. Rev. E **47**, 2606 (1993).
[4] C. J. Rueb and C. F. Zukoski, J. Rheol. **42**, 1451 (1998).
[5] S. A. Shah, Y. L. Chen, K. S. Schweizer, and C. F. Zukoski, J. Chem. Phys. **119**, 8747 (2003).
[6] J. F. Brady, J. Fluid Mech. **272**, 109 (1994).
[7] A. T. J. M. Woutersen, J. Mellema, C. Blom, and C. G. Dekruif, J. Chem. Phys. **101**, 542 (1994).
[8] M. A. Bevan, S. N. Petris, and D. Y. C. Chan, Langmuir **18**, 7845 (2002).
[9] M. A. Bevan and D. C. Prieve, Langmuir **16**, 9274 (2000).
[10] D. W. Marr and A. P. Gast, J. Chem. Phys. **99**, 2024 (1993).
[11] S. B. Lee, J. Chem. Phys. **114**, 2304 (2001).
[12] Y. C. Chiew and E. D. Glandt, J. Phys. A **16**, 2599 (1983).
[13] N. F. Carnahan and K. E. Starling, J. Chem. Phys. **51**, 635 (1969).
[14] J. F. Brady and G. Bossis, Annu. Rev. Fluid Mech. **20**, 111 (1988).
[15] D. J. Jeffrey and Y. Onishi, J. Fluid Mech. **139**, 261 (1984).
[16] D. L. Ermak and J. A. McCammon, J. Chem. Phys. **69**, 1352 (1978).
[17] R. J. Phillips, J. F. Brady, and G. Bossis, Phys. Fluids **31**, 3462 (1988).
[18] A. J. C. Ladd, J. Chem. Phys. **93**, 3484 (1990).
[19] J. F. Brady, J. Chem. Phys. **98**, 3335 (1993).